Asia-Pacific Journal of Science and Technology: Volume: 30. Issue: 03. Article ID.: APST-30-03-04. Research Article

APST

Asia-Pacific Journal of Science and Technology

https://www.tci-thaijo.org/index.php/APST/index

Published by Research Department,
Khon Kaen University, Thailand

# Electrospun chitosan/polyvinyl alcohol nanofibrous membrane loading curcumin to promote wound healing and improve antibacterial properties

Ngoc-Hanh Cao-Luu[1,2,*], Bich-Thuyen Nguyen-Thi[1], Huynh-Vu-Thanh Luong[1,3], Lien-Huong Huynh[1], Thuy-Tien Tiet-Thi[2], and Kim-Oanh Nguyen-Thi[2]

[1]Faculty of Chemical Engineering, Can Tho University, Can Tho 900000, Vietnam
[2]Composite Material Laboratory, Faculty of Chemical Engineering, Can Tho University, Can Tho 900000, Vietnam
[3]Applied Chemical Engineering Laboratory, Faculty of Chemical Engineering, Can Tho University, Can Tho 900000, Vietnam
[*]Corresponding author: clnhanh@ctu.edu.vn

Received 25 October 2023
Revised 28 August 2024
Accepted 25 September 2024

**Abstract**

Wound healing nanofiber membranes were successfully fabricated by electrospinning of chitosan (CS) and polyvinyl alcohol (PVA) solution in the presence of curcumin (CCM). As a results, the optimal material parameters included 2% (w/v) for the CS concentration, 8% (w/v) for the PVA concentration, 3% for the CCM concentration (by mass of CS), 3/7 for the CS/PVA volume ratio; the process parameters of 15 cm for the needle tip-to-collector distance, 15 kV for the applied voltage, and 0.1 mL/h for the solution flow rate. The obtained membranes exhibited the relatively uniform diameter fibers distributed from 200 to 450 nm, average diameter at 348.55 ± 51.48 nm, smooth fiber surface, and uniform fiber texture. The fourier transform infrared spectroscopy (FTIR) results demonstrated the presence of CCM in the CS/PVA/CCM membrane, thereby showing that the structure of CCM is not changed during the fabrication. *In-vitro* test showed that the amount of CCM released significantly from CS/PVA/CCM membrane during the first 6 hours (up to 80.28%), it was followed by maintain at a rather slow rate, and the maximum CCM released was 92.26% after 72 h. The prepared CCM membrane exhibits high antibacterial activity against Gram-negative (*Escherichia coli*) and Gram-positive (*Listeria monocytogenes*) bacteria strain, which is an important property of wound healing membrane. Remarkably, CS/PVA/CCM nanofiber membrane accelabrates healing process in rats with incised wounds and demonstrates superior healing ability comparing to CS/PVA membrane and commercial bandages. In brief, CS/PVA/CCM nanofiber membrane is a potential wound dressing with good healing and high antibacterial properties.

**Keywords:** Chitosan, Curcumin, Electrospinning method, Polyvinyl alcohol, Wound healing nanofibrous membranes

## 1. Introduction

Skin is an essential organ in the human body that serves as a protective barrier and first line of defense against environmental elements [1]. It serves an important function in preventing harmful agents and microorganisms from invading the body [2]. However, skin is a sensitive organ that is easily injured by external impacts. Indeed, it is difficult for humans to avoid impacts on their bodies, resulting in the production of many forms of skin wounds, the most prevalent of which are open wounds. Open wounds are the portal for bacteria to enter the body, which if not cleaned and treated appropriately can lead to significant problems such as infection or even death [3]. As a result, when skin is damaged by an open wound, it must be covered quickly with an adequate dressing to provide hemostatic support and accelerate healing [4]. Thus, many studies have been undertaken to develop new therapeutic systems that aid in the wound healing process [5,6]. Currently, nanostructured fibrous membranes fabricate from natural and synthetic biopolymers are gaining popularity [7]. Nanofibers with a large specific surface area can induce hemostasis while also maintaining a proper moist environment for the injury by allowing

oxygen penetration and fluid buildup, hence increasing protection [8]. Furthermore, nanofibrous membranes may successfully shield wounds from microbiological invasion and are easily combined with therapeutic compounds. [8]. Furthermore, wound healing membranes must have several essential properties, including (1) adequate water vapor permeability to keep the surrounding physiological environment moist around the incision, (2) increased air permeability, (3) good liquid adsorption, (4) an external bacterial protection barrier, (5) antimicrobial properties to prevent bacterial infections, and (6) no cytotoxic elements in the event that neonates sustain additional damage [8].

This work attempted to construct an electrospun nanocomposite membrane incorporating a therapeutic ingredient as an innovative dressing for accelerating wound healing. The nanofibrous membrane is made from chitosan (CS), a natural degradable polymer, with the addition of polyvinyl alcohol (PVA), an electro-spinnable polymer, and is integrated with curcumin (CCM), a bioactive molecule, using the commonly utilized electrospinning technique for wound dressing applications. Electrospun nanofibrous composite membranes made from natural and synthetic biopolymers have been found to benefit from the biological features of natural biopolymers while also having higher mechanical properties and slower degradation rates than synthetic polymers [9,10].

CS is a natural biopolymer with a linear structure made of N-acetyl-D-glucosamine units and D-glucosamine units connected by β-(1-4) glycosidic linkages (Figure 1). CS is a promising material for wound dressing formulation due to its inherent antimicrobial activity [10], biocompatibility [11], biodegradability with non-toxic residues [12], and wound healing benefits [13]. It has been demonstrated that N-acetyl glucosamine, as a monomer unit of CS, induces hemostasis, promotes cell proliferation, and hence accelerates wound healing [14]. In the event of hypertrophic scar development, which is defined by excessive collagen production during the remodeling phase, CS can reduce scar tissue, allowing for successful re-epithelialization [15]. Although CS-based wound dressings show potential for biomedical applications, their stiff structure, strong hydrogen bonding, non-thermoplastic behavior, and high crystallinity result in low mechanical characteristics, which were often a hurdle in the electrospinning process [16]. As a result, the combination of CS with an electrospinnable polymer, such as PVA, can address these issues.

PVA is a synthetic polymer with many hydroxyl groups in its structure, making it a water-soluble substance [17]. Furthermore, PVA exhibits important wound healing qualities such as biocompatibility, biodegradability, and nontoxicity [17]. Furthermore, because of its high electrospinnability, PVA is commonly employed to supplement CS natural polymer in the production of nanofibers [10]. The combination has good mechanical and chemical properties because of its unique intermolecular interactions based on chemical structure and physical characteristics [18]. The interactions discovered between amino groups in the CS structure and hydroxyl groups in the PVA formulation were hydrogen bonding and electrostatic interactions, which contribute to the physical cross-linking of the polymer network [19]. These unique features of materials may boost tensile strength and toughness while maintaining the shape and structure integrity of the mats and optimizing the biodegradation rate during the wound healing process [20].

To improve the open wound healing capabilities of nanofibrous membranes made from active polymers, CCM, a natural medicinal ingredient, is inserted into the healing membrane as a therapeutic agent. CCM, a lipophilic bioactive molecule found in turmeric (*Curcuma longa*) rhizome [21], has remarkable anti-inflammatory, antioxidant (free radical scavenging), and anti-microbial activities [22]. Furthermore, CCM has been shown to be both safe and effective in humans, with significant modifying effects on wound healing [23]. CCM's efficacy for wound healing stems mostly from its capacity to promote granulation tissue formation, collagen deposition, tissue remodeling, and wound contraction, making it a suitable chemical for healing applications. Unfortunately, CCM's original form is limited due to its low bioavailability, quick metabolism, poor solubility, and light sensitivity [24]. As a result, integrating CCM into the CS/PVA nanofibrous membrane has the potential to address its shortcomings while also increasing its therapeutic potential.

The major purpose of this study was to improve the wound healing and antibacterial properties of an electrically spun CS/PVA nanofibrous membrane utilizing CCM in combination. The factors affecting the electrospinning process, such as reagent concentration and ratio, were examined to identify the optimal conditions. The shape of composite nanofibers was evaluated, as well as their diameter. FTIR was employed to detect drug-polymer and polymer-polymer interactions in fiber compositions. The CCM's release from the hybrid nanofibrous forms was determined. Two bacteria, namely *Listeria monocytogenes* and *Escherichia coli* , were used to assess the antibacterial performance of the samples. The nanofibrous membrane samples were fabricated under optimal conditions and the control samples were examined on a mouse model.

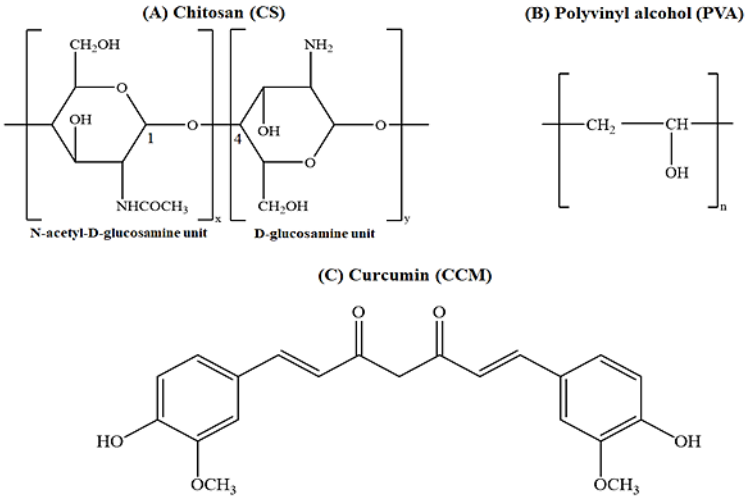


**Figure 1** Chemical structure of (A) CS, (B) PVA, and (C) CCM.

## 2. Materials and methods

### *2.1 Materials*

In this work, chemicals such as CS (CS, deacetylation at 92%, Viet Nam), PVA (PVA, 99.5%, Xilong, China), CCM (CCM, >90%, Viet Nam), acetic acid (AA, 90%, Jinhuada, China), phosphate buffered saline (PBS, Himedia, India), ethanol (95%, Chemsol, Viet Nam) were used. Gram-negative *E. coli* and Gram-positive *L. monocytogenes* were employed. All other materials and reagents applied in this work were of a grade for analysis.

### *2.2 Fabrication of CS/PVA/CCM nanofiber membranes*

The steps to prepare CS/PVA/CCM solution are shown in Figure 2. Firstly, dissolving 8 g of PVA in 100 mL of deionized water, the mixture was then magnetically stirred at 80°C for 4 hours to obtain an 8% (w/v) PVA homogenous solution. Next, the CS powder was dissolved in a 10% (v/v) acetic acid solution and stirred overnight at room temperature to create a 2% (w/v) by weight CS solution [25]. Afterwards, CS solution and 3% CCM (by mass of CS) were combined, and the mixture was stirred for 1 hour to generate the CS/CCM solution. Finally, the CS/CCM and PVA solutions will be mixed together in varying volume ratios (1:9, 2:8, 3:7, 4:6, 5:5, 6:4) and stirred for 1 hour to acquire a homogeneous mixture. A 1 mL syringe was filled with the prepared solution and followed by connected to a stainless steel needle. During electrospining process, the pump speed is adjusted at 0.1, 0.2, and 0.3 mL/h and voltages of 13, 15, and 17 kV are applied to the needle's tip and the collector, the distance from the needle tip to the sample collector is changed from 14 to 15 and 16 cm.

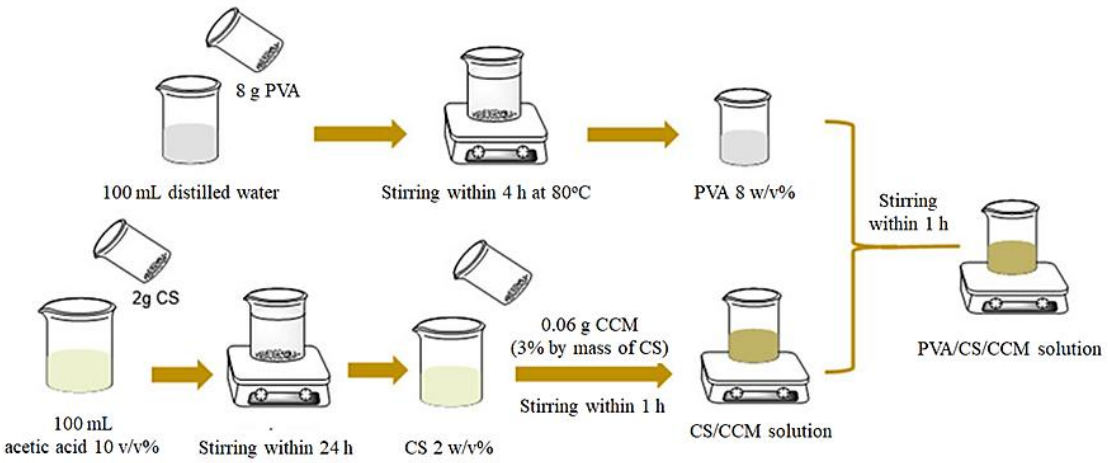


**Figure 2** Diagram of CS/PVA/CCM solution preparation.

*2.3 Characterization of nanofiber membranes*

*The morphology, diameter, and size distribution of nanofibers*

For the pre-tests, the diameter of the nanofibers was determined using an optical microscope (Nikon EPIPHOT 200, Japan). The nanofibers gathered on the aluminum film directly and observed by Hitachi S-4800, a scanning electron microscope made in Japan. To improve their observation, the nanofibers were sputter-coated with a platinum layer prior to measurement. Using ImageJ software, the results of scanning electron microscope (SEM) images were used to calculate the fiber average size and fiber size distribution.

*Fourier transform infrared spectroscopy (FTIR)*

To describe the specific functional groups found in the nanofibrous membrane, Fourier transform infrared (FTIR) instrument (Nicolet 6700, Thermo, USA) was utilized. Under nitrogen flow, the FTIR spectrum was captured with a total of 32 scans and a resolution of 4 $cm^{-1}$ in the wavenumber range 4000-400 $cm^{-1}$.

*2.4 In-vitro release of CCM*

A standard curve for the quantification of CCM was prepared. A desired amount of 0.005 g standard CCM was accurately weighed and placed in a volumetric flask with a 4:1 mixture of ethanol and PBS buffer. By adding 1, 2, 3, 4, and 5 mL of this standard solution to a volumetric flask, a solution with concentrations of 0.002, 0.004, 0.006, 0.008, and 0.01 mg CCM/mL was prepared. The absorbance (A) of these solutions was measured at the maximum wavelength ($\lambda_{max}$ = 425 nm). The measured values are plotted to show the correlation between A and C, a linear relationship of A according to C is obtained. The above equation is used to calculate the CCM concentration in the test. From the obtained standard curve equation, for each test sample, the amount of CCM released during the *in-vitro* experiment will be calculated, thereby calculating the proportion of CCM released from the nanofiber membrane.

The CCM content released from nanofiber membranes was determined. To simulate animal serum medium, approximately 5 mg of CS/PVA/CCM membranes with a CS/PVA ratio of 3:7 and 3% CCM by mass of CS was first mixed with 10 mL of PBS (pH 7.4) and 1% tween 20 in a glass-stoppered glass vial. The sample vials were maintained at 37 ± 1°C. Following that, 2 mL of sample was withdrawn for analysis and 2 mL of fresh buffer was added at 5 min, 10 min, 15 min, 30 min, 1 h, 2 h, 3 h, 4 h, 6 h, 12 h, 24 h, 48 h and 72 h intervals. The withdrawn sample of 2 mL was mixed with an ethanol solution of 8 mL to dissolve the amount of CCM in the buffer and then examined by a Labomed spectrophotometer (UV-VIS, UVD-3500, USA) to determine the amount of CCM released. CCM release percentage was calculated as follows Equation (1):

$$\%\ \text{curcumin release} = \frac{amount\ of\ curcumin\ release\ at\ t}{amount\ of\ curcumin\ in\ fiber\ membrane}\ x\ 100\% \quad (1)$$

*2.5 Antibacterial evaluation assay*

The agar disk diffusion method was used to test the antibacterial activity against *L. monocytogenes* and *E. coli*. These strains of bacteria were grown in liquid Luria-Bertani (LB) medium for 24 to 48 h at 37°C. This is followed by an overnight incubation, and titrated McFarland 0.5 with 0.85% physiological saline solution. The optimum CS/PVA/CCM and CS/PVA nanofiber membrane samples were cut into 1 cm diameter circular pieces. The positive and negative controls were also prepared for comparison. The antimicrobial activity of the samples was determined using the Kirby-Bauer method. 100 µL of bacterial suspension (5 x $10^6$ CFU/mL) was spread evenly on a petri dish containing liquid LB medium. Circular samples were positioned on the agar layer's surface in a petri dish. The experiment was triplicated on the same plate. After that, the plates were put in a 37 °C incubator for 24 h. Finally, the antimicrobial activity results were recorded via measuring the diameter of the sterile ring.

*2.6 In-vivo wound healing ability assay*

For animal study, healthy female mice with the average weight of 40-45 g were chosen and placed in an experimental room for 7 days to release stress and familiar with room environment before inducing wound. The mice were anesthetized with ether, followed by having their backs shaved and a 1 cm long skin wound. The mice were divided into four groups. Group 1 was untreated (control sample), group 2 was treated with commercial bandage, group 3 was treated with PVA-CS membrane, and group 4 was treated with CS/PVA/CCM membrane. To assess the length of a healing wound, the length of the wound was measured over 12 days with a ruler. On the

0, 3rd, 6th, 9th, and 12nd day, the wounds were photographed. The number of days required to not have any raw wound left was defined as the time it took for the wound to heal.

## 3. Results and discussion

### *3.1 Results of the factors influencing the electrospray process*

The influence of CS/PVA ratios on fiber formation was investigated via optical microscope images of CS/PVA nanofibrous membranes (Figure 3). The CS content in the solution was gradually increased in this study, resulting in a steady increase in fiber diameter. When the CS/PVA ratio is greater than 6:4, fibers were not formed and there was a grainy appearance. This is because CS is an electrolyte polymer, so the conductivity of the solution increases as its concentration increases. This results in a higher charge at the solution surface being sprayed out of the needle tip during electrolysis. As the number of charged nanofibers ejected from the needle tip increases, a higher tensile force is required to continue pulling the yarn as a result of an electric field's action. Therefore, the overall pulling force of the fibers depends on the self-repulsion of the charges at the needle tip, so as the charge density increases, the fiber diameter will be small [26].

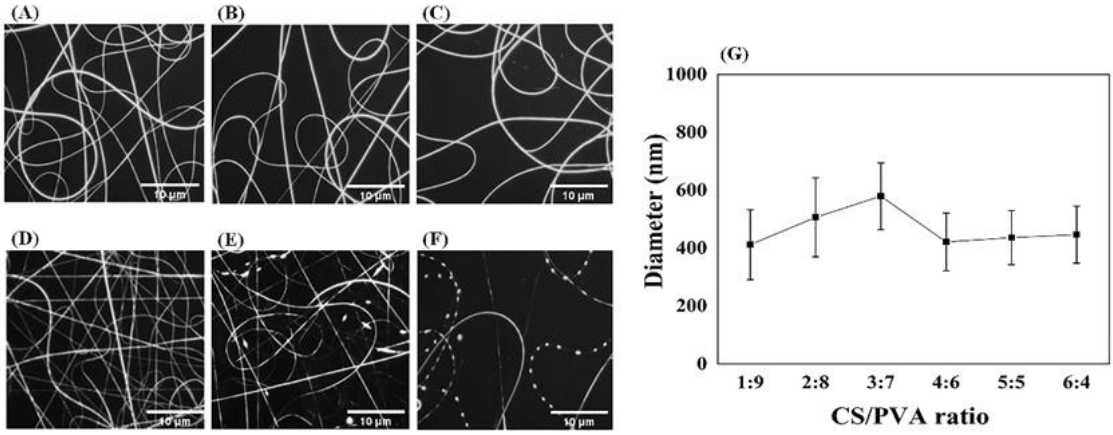


**Figure 3** Optical microscope images of CS/PVA fibers at different volume ratio of (A) 1:9, (B) 2:8, (C) 3:7, (D) 4:6, (E) 5:5, (F) 6:4 and (G) corresponding diameter graph.

The results of investigating the effect of CCM concentration were shown in Figure 4 through optical microscope images of CS/PVA/CCM fiber membrane. The addition of CCM reduced the average size of the nanofibers as illustrated in Figure 4D. At the CCM concentration 1%, nanofibers had the largest diameter and fibers containing 5% CCM had the smallest diameters. This result may be due to the increase in conductivity of the solutions with increasing CCM content. Because of the increased electrical conductivity, the solution can be stretched more easily, resulting in a narrowing of the fiber diameter. Therefore, the addition of CCM can enhance the conductivity of the solution and thereby reduce the fiber diameter [26]. The results showed that the fiber containing 5% CCM had the smallest diameter, but a small amount of CCM deposited at the bottom of the solution when pulling out. Therefore, the optimal concentration of CCM was selected as 3% because of the large fiber diameter at 1% concentration and incompletely dissolved of CCM at 5%.

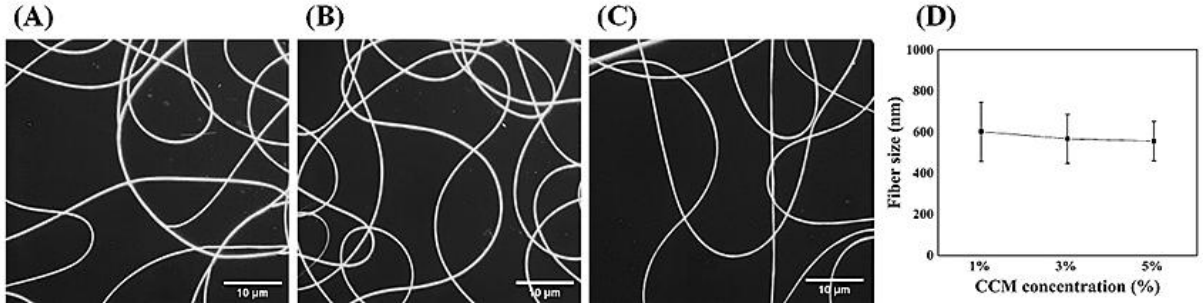


**Figure 4** Optical microscopy images of CS/PVA/CCM fibers with varying CCM concentration: (A) 1 w/v%, (B) 3 w/v%, (C) 5 w/v% and (D) corresponding diameter graph.

The optical microscopy results of CS/PVA/CCM fibers with different distances from the needle tip to the sample collector of 14, 15, and 16 cm were showed in Figure 5. Among the three samples, the fibers fabricated at

a distance of 15 cm had the smallest diameter and uniform diameter distribution. At a distance of 14 cm, the obtained fibers had a large diameter and fiber size heterogeneity was clearly displayed. When increasing distance to 15 cm, the fiber size tends to decrease because the long-distance leads to a longer evaporation time resulting in a smaller fiber diameter. Besides, the longer distance of 16 cm caused the solution instability at the needle tip increasing the fiber size distribution [27]. Therefore, to obtain the optimal CS/PVA/CCM fiber, a distance of 15 cm was chosen.

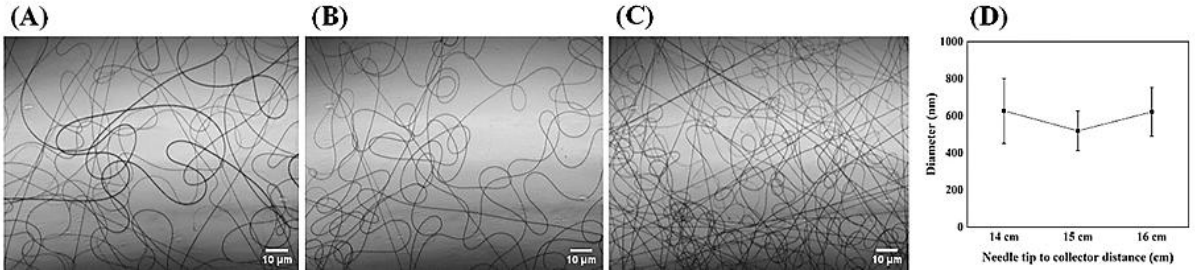


**Figure 5** Optical microscope images of CS/PVA/CCM fibers with different distances from the needle tip to the sample collector of (A) 14 cm, (B) 15 cm, (C) 16 cm and (D) corresponding diameter graph.

Figure 6 showed the effect of applied voltage through optical microscopy images of CS/PVA/CCM fibers at various levels of voltage (e.g. 13 kV, 15 kV, and 17 kV) applied to CCM of 3 w/v%, distance between the tip of the needle and the collector of 15 cm, a solution flow rate of 0.1 mL/h. In general, as the applied voltage was raised to 17 kV, the fiber diameter decreased. This is attributed to increase in the voltage causing a stronger the pulling force, which leads to prolong the fibers, thereby reduces the fiber diameter [27]. Therefore, the smallest fiber diameter was obtained at 17 kV; however, the fiber diameter did not show a uniform distribution. At the voltage of 13 kV, the larger diameter fibers were obtained and many dripping spots appeared. At 15 kV, the fibers had a relatively uniform size. Therefore, the voltage of 15 kV was suitable for further experiments.

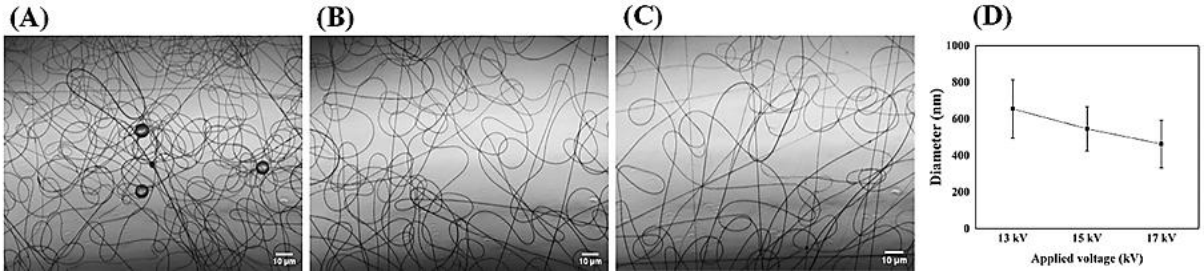


**Figure 6** Optical microscope images of CS/PVA/CCM fibers at various voltage values: (A) 13 kV, (B) 15 kV, (C) 17 kV and (D) corresponding diameter graph.

The results of solution flow rate effect are shown in optical microscope images (Figure 7). CS/PVA/CCM filaments were synthesized at varying flow rates of 0.1, 0.2, and 0.3 mL/h. The obtained nanofiber at 0.1 mL/h showed the best morphology and the relatively uniform distribution of fiber diameter. At higher flow rate of 0.2 mL/h and 0.3 mL/h, the resulting fibers are dripped resulting in agglomeration of the fibers. The reason is that when the speed is high, the amount of solution is pushed out quickly, resulting in large fibers and dripping [27]. Therefore, the optimal flow rate is 0.1 mL/h.

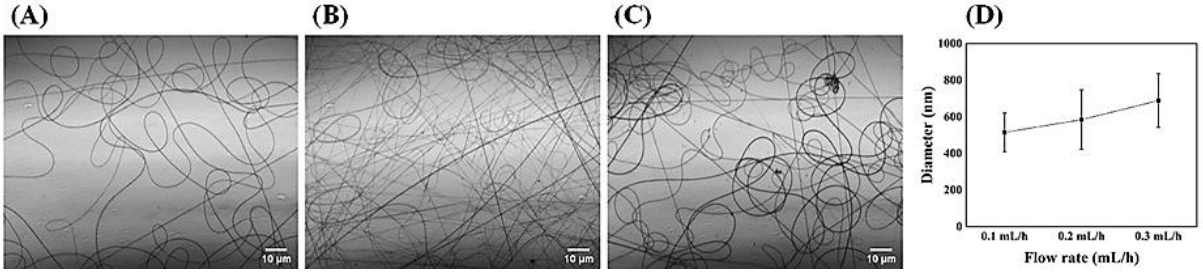


**Figure 7** Optical microscope images of CS/PVA/CCM fibers at different speed: (A) 0.1 mL/h, (B) 0.2 mL/h, (C) 0.3 mL/h and (D) corresponding diameter graph.

*3.2 Morphology of electrospun nanofibers*

Figure 8 shows a scanning electron microscope image of CS/PVA/CCM fiber film with optimal conditions such as CS/PVA ratio of 3:7, CCM content of 3%, distance from needle tip to sample collection of 15 cm, the voltage applied of 15 kV and the flow rate of 0.1 mL/h. The results show that the average fiber diameter is at 348.55 ± 51.48 nm and the diameter distribution is in the range from 200 to 450 nm, mostly in 400 nm. In addition, no particles can be observed on the fiber surface, which indicates that the CCM completely dissolved in the polymer solution. Compared with the electrospinning study of poly lactic acid (PLA)/CCM nanofibers by Thuy et al (2013) [28], the diameter of CS/PVA/CCM fibers is significantly smaller than that of PLA/CCM fibers. In PLA/CCM fibers with CCM ratios of 0.125%, 1.250% and 6.250%, the fiber diameters are 943 ± 383 nm, 666 ± 130, and 562 ± 177 nm, respectively while the CS/PVA/CCM fiber diameters in this study are 348.55 ± 51.48 nm [28].

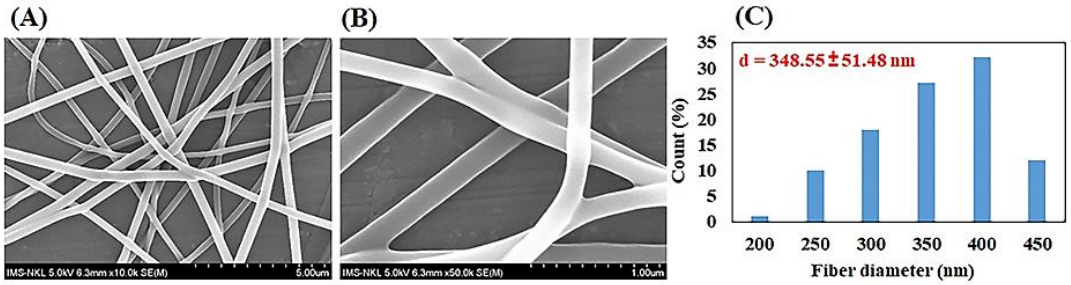


**Figure 8** The SEM images in different scales: (A) x10,000, (B) x50,000; and (C) fiber diameter distribution histograms of CS/PVA/CCM nanofibrous membrane under optimal conditions.

Figure 9 showed the results of the specific functional groups presented in the nanofiber membrane through FTIR spectroscopy analysis of CCM, CS/PVA membrane (the volume ratio of CS:PVA = 3:7), and CS/PVA/CCM membrane (the volume ratio of CS:PVA = 3:7, 3% CCM). The results showed that the CS/PVA/CCM membrane had a shift of the peaks when CCM was added to the CS/PVA mixture to fabricate the membrane. Specifically, the 3,298 $cm^{-1}$ peak corresponded to the stretching oscillations of two hydroxyl group (-OH) of CS, PVA, CCM and amino (-NH) of CS, which shifted to a lower wavenumber. This indicated that there was a hydrogen bond formation between the hydroxyl groups in the CS, PVA chains and the hydroxyl groups in the CCM [29]. In addition, some characteristic peaks of CCM in the CS/PVA/CCM membrane showed a non-phase separation from the original, demonstrating the presence of CCM in the fibrous membrane. Indeed, the peaks 1,429 $cm^{-1}$ and 1,374 $cm^{-1}$ were the alkanes (-CH) of CCM in the CS/PVA/CCM membrane shifted from the 1428 $cm^{-1}$ and 1376 $cm^{-1}$ peaks of the alkanes of the original CCM. This change in band intensity was due to PVA's tendency to develop a binding to water and to the hydroxyl group presented in CS and CCM [29]. The appearance of the ether (-CO) group at the bands of 1,255 $cm^{-1}$ and 1,093 $cm^{-1}$ in the CS/PVA/CCM fibrous membranes referred to the displacement and binding overlap relative to the peaks of 1,205 $cm^{-1}$, 1,114 $cm^{-1}$, 1027 $cm^{-1}$ (-CO of CCM) and 1,089 $cm^{-1}$ (-CO of CS/PVA membrane). Besides, the appearance of the 1,715 $cm^{-1}$ peak (C=O group) was related to the association overlap compared with the peak of C=O group of the CS/PVA membrane at 1,716 $cm^{-1}$ and of the CCM at 1,625 $cm^{-1}$ [29]. In summary, the FT-IR results of CCM, CS/PVA film and CS/PVA/CCM film confirmed a successful fabrication of PVA, CS and CCM by electrospinning method due to the interaction and compatibility between the polymer and CCM to be suitable for the incorporation process, but still retain the structure of CCM.

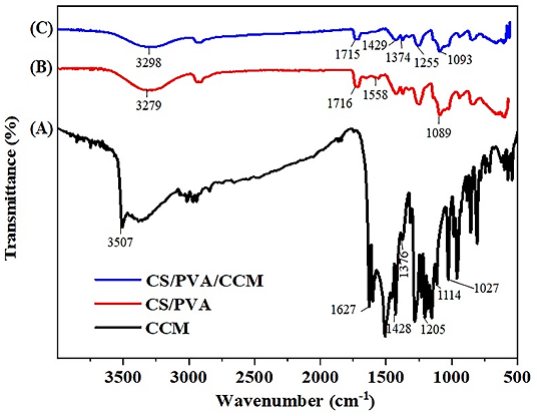


**Figure 9** The FT-IR spectrum of (A) CCM, (B) CS/PVA nanofibrous membrane, (C) CS/PVA/CCM nanofibrous membrane.

*3.3 Results of in-vitro drug delivery*

The amount of drug released was calculated using a calibration curve generated by a UV-Vis instrument scanning at the CCM maximum wavelength of 425 nm using a standard curve equation y = 0.1150x + 0.0215 ($R^2$ = 0.9984) in pH 7.4. The process of CCM release in the buffer solution of wound healing membrane from CS/PVA/CCM nanofibers is depicted in Figure 10A.

Due to the hydrophilic characteristic of CS and PVA, diffusion of CCM molecules induced when introducing the membrane into the release medium, so that the amount of CCM released increased significantly at the initial stage. The mechanism of CCM release from membrane were diffusion mechanism, CCM molecules diffused from CS/PVA/CCM membrane to the release medium via concentration gradient. As a result, at the first 6 hours, the amount of released CCM increased quickly, up to 80.28% as shown in Figure 10B. After 6 hours, the amount of released CCM maintained at a relatively slow rate and the highest percentage of CCM released at 72 h was 92.26% which was greater than the outcomes of Mahmud et al' study in 2020 (the maximum percentage of CCM released from PVA/CCM fibers at 24 hours was 72%) [30].

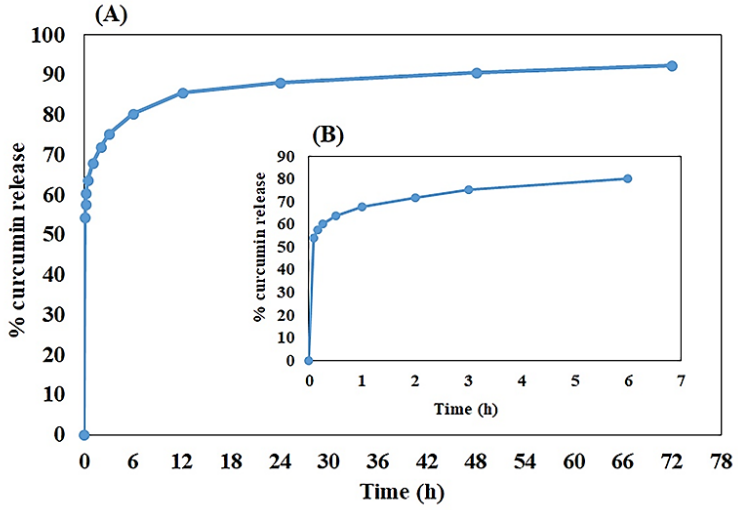


**Figure 10** CCM release profile from CS/PVA/CCM incubation at 37 °C in (A) 72 hours and (B) 6 hours.

*3.4 Antibacterial property assessments*

The antibacterial property of prepared CS/PVA and CS/PVA/CCM nanofibrous membrane tested against *E. coli* and *L. monocytogenes* using the disc diffusion method (Figure 11). As a result, the inhibitory zone for the CS/PVA sample were 12.667 ± 0.577 mm (Figure 11A) and 14.167 ± 0.764 mm (Figure 11E) for *E. coli* and *L. monocytogenes*, respectively. By adding 3% of CCM, the growth inhibition zone diameter of CS/PVA/CCM sample increased to 17.233 ± 0.252 mm (Figure 11B) and 17.167 ± 0.208 mm (Figure 11F) for *E. coli* and *L. monocytogenes*, respectively. Therefore, the novel CS/PVA/CCM nanofibrous membrane with a combination of CS and CCM exhibited promising antibacterial activity against all tested microorganism.

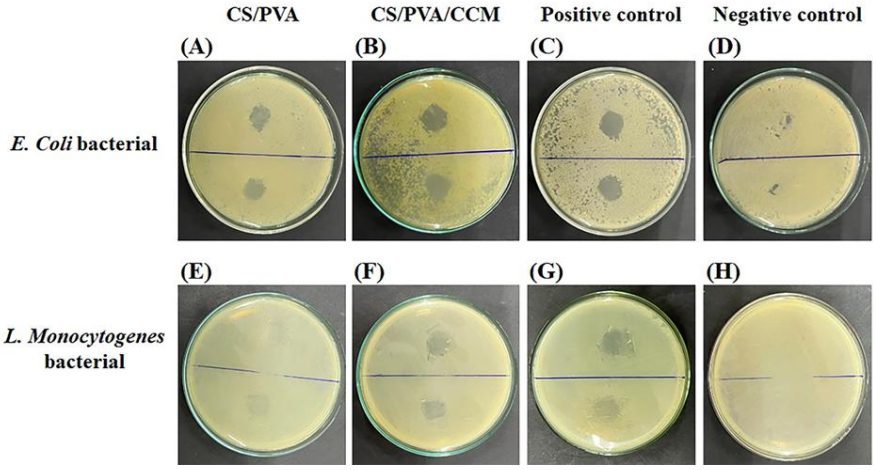


**Figure 11** Antibacterial activity of (A,E) CS/PVA, (B,F) CS/PVA/CCM, (C,G) positive, and (D,H) negative control sample against *E. Coli* and *L. Monocytogenes* bacterial.

*3.5 Evaluation of the wound healing ability in-vivo*

The wound healing ability of CS/PVA/CCM membranes was investigated through wounding in mice, observing the wound healing process, and comparing with control samples (the self-healed wound, commercial bandage, and CS/PVA). The changes of wound in mice were observed on various time intervals of 0, 3, 6, 9 and 12 days after the wound formation (Figure 12).

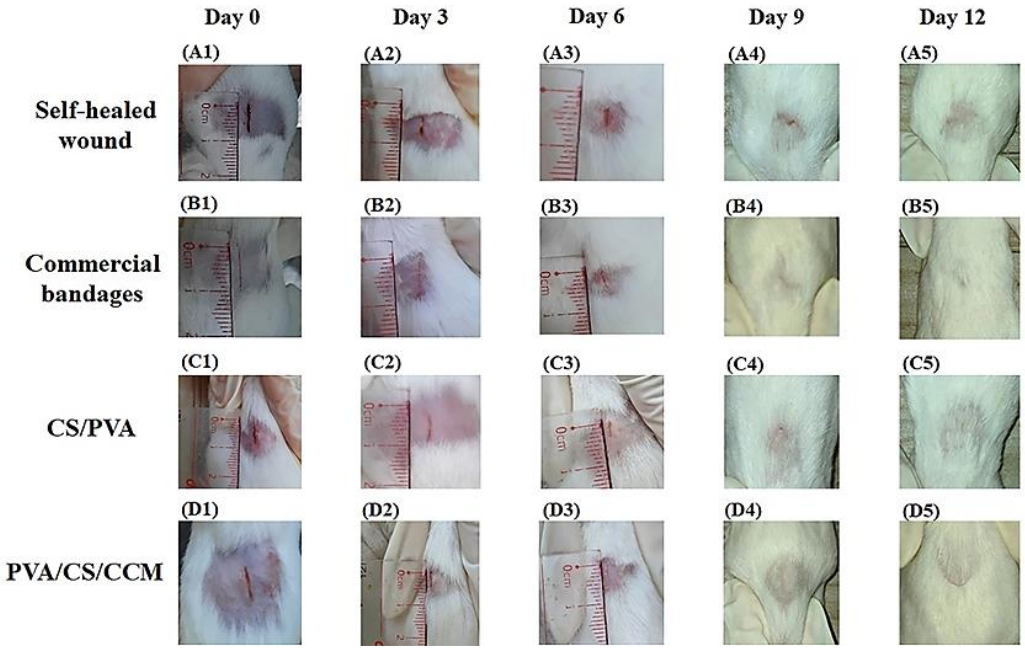


**Figure 12** Pictorial representation of wound reduction for (A) control samples (the self-healed wound) and after treatment with (B) commercial bandage, (C) CS/PVA, (D) CS/PVA/CCM at different time points.

As a result, the wounds applied CS/PVA/CCM membranes significantly improved wound closure ability compared with wounds treated with CS/PVA membranes, commercial bandage and self-healing wounds. On the day 3, wounds in mice treated CS/PVA/CCM were assessed to be minimal, without bleeding or exudation. This may be due to the anti-inflammatory, antibacterial, and tissue-regenerating effects of CCM. Besides, wounds treated with commercial bandage have a good healing ability but slower than those treated with CS/PVA/CCM membranes. The wound applied CS/PVA membrane stopped bleeding but still quite large due to the hemostatic ability and cell proliferation ability of CS while there were still some open wounds and bleeding for the self-healed wound. After 6 days, wounds treated with CS/PVA/CCM membranes showed almost complete healing, wounds treated with commercial bandage and CS/PVA fibrous membranes healed significantly. The self-healing wounds were no longer bleeding and partially closed. At the day 9, the wounds in mice treated with both commercial bandage and CS/PVA fibrous membranes were almost completely healed while the self-healing mouse still had some small openings. On the 12th day, the wounds in all 4 groups of mice completely healed. Consequently, the group of mice applied CS/PVA/CCM membranes needed 6 days to close the wound completely; meanwhile, it took 9 days for wounds treated with commercial bandages and CS/PVA membranes healing. This result is consistent with the findings of Dhurai et al., 2013 [26] and Thuy et al., 2013 [28]. It can be seen that CS/PVA/CCM membranes have better wound healing ability than the control samples. In other words, the membrane combining CS, PVA, and CCM has great potential in wound healing.

## 4. Conclusion

With the optimal parameters (2% (w/v) for the CS concentration, 8% (w/v) for the PVA concentration, 3% for the CCM concentration by mass of CS, 3/7 for the CS/PVA volume ratio, 15 cm for the needle tip-to-collector distance, 15 kV for the applied voltage, and 0.1 mL/h for the solution flow rate), the produced CS/PVA/CCM membrane possessed smooth fibrous surface and it was in a relatively uniform diameter distributed in ~200-450 nm with average diameter at 348.55 ± 51.48 nm. The physical crosslinking formation between the CS amide group and PVA hydroxyl group and the presence of CCM in the polymer network were confirmed through FTIR results. *In vitro* release data of CS/PVA/CCM membrane exhibited effective CCM release capacity with cumulative release above 90%. The supplementation of CCM into the membrane showed stronger antibacterial activity against *L. monocytogenes* and *E. coli* compared to non-CCM polymeric membranes. Furthermore, the superior

effect of CS/PVA/CCM membrane in the treatment of wounds on mice, compared with commercial bandages, CS/PVA membranes, and self-healed wounds was demonstrated. The wound healing time treated with CS/PVA/CCM membranes in mice was about 6 days, only half the time compared to self-healing wounds. Overall, the results indicated that CS/PVA/CCM nanofibrous membrane has great potential in the healing of open wounds. Despite some success outcomes from such approaches, further investigations are required to elucidate the long-term beneficial and adverse effects to make use of them for clinical applications. The investigations of cellular biocompatibility, implementation of cell uptake studies, carrying out in vivo bioavailability, and employment of histological evaluation of wounds should be assessed carefully through further research.

## 5. Ethical approval

Ethical approval was granted by the Council for Science and Education, Can Tho University (The approval reference number: BQ2023-01/TBK) prior to experimentation. All animal experimentation was conducted in accordance with accepted standards of humane animal care, as outlined in the Ethical Guidelines of the National Health and Medical Research Council.

## 6. Acknowledgements

This work is supported by funding from Can Tho University, Vietnam. Grant number: T2023-98. Special thanks to Ms. Tuong-Vy Nguyen at Composite Material Laboratory, Can Tho University for the experimental supports.

## 7. Conflicts of interest

The authors declare that there is no conflict of interest.

## 8. References

[1] Chen K, Hu H, Zeng Y, Pan H, Wang S, Zhang Y, Shi L, Tan G, Pan W, Liu H. Recent advances in electrospun nanofibers for wound dressing. Eur Polym J. 2022;178:111490.

[2] Pereira RF, Barrias CC, Granja PL, Bartolo PJ. Advanced biofabrication strategies for skin regeneration and repair. Nanomedicine. 2013;8(4):603-621.

[3] Zhou S, Xie M, Su J, Cai B, Li J, Zhang K. New insights into balancing wound healing and scarless skin repair. J Tissue Eng. 2023;14.

[4] Liu C, Zhu Y, Lun X, Sheng H, Yan A. Effects of wound dressing based on the combination of silver@ CCM nanoparticles and electrospun CS nanofibers on wound healing. Bioengineered. 2022;13(2): 4328-4339.

[5] Rath G, Hussain T, Chauhan G, Garg T, Goyal AK. Collagen nanofiber containing silver nanoparticles for improved wound-healing applications. J Drug Target. 2016;24(6):520-529.

[6] Croitoru AM, Ficai D, Ficai A, Mihailescu N, Andronescu E, Turculet SC. Nanostructured fibers containing natural or synthetic bioactive compounds in wound dressing applications. Materials. 2020;13(10):2407.

[7] Chen J, Tang X, Wang Z. Techniques for navigating postsurgical adhesions: Insights into mechanisms and future directions. Bioeng Transl Med. 2023;10565.

[8] Gomes SR, Rodrigues G, Martins GG, Roberto MA, Mafra M, Henriques CMR, Silva JC. *In vitro* and *in vivo* evaluation of electrospun nanofibers of PCL, CS and gelatin: A comparative study. Mater Sci Eng C. 2015;46:348-358.

[9] Adeli H, Khorasani MT, Parvazinia M. Wound dressing based on electrospun PVA/CS/starch nanofibrous mats: Fabrication, antibacterial and cytocompatibility evaluation and in vitro healing assay. Int J Biol Macromol. 2019;122:238-254.

[10] Matica MA, Aachmann FL, Tøndervik A, Sletta H, Ostafe V. CS as a wound dressing starting material: Antimicrobial properties and mode of action. Int J Mol Sci. 2019;20(23):5889.

[11] Jana P, Shyam M, Singh S, Jayaprakash V, Dev A. Biodegradable polymers in drug delivery and oral vaccination. Eur Polym J. 2021;142:110155.

[12] Saghazadeh S, Rinoldi C, Schot M, Kashaf SS, Sharifi F, Jalilian E, Khademhosseini A. Drug delivery systems and materials for wound healing applications. Adv Drug Deliver Rev. 2018;127:138-166.

[13] Bi H, Feng T, Li B, Han Y. In Vitro and In Vivo Comparison Study of Electrospun PLA and PLA/PVA/SA Fiber Membranes for Wound Healing. Polymers. 2020;12:839.

[14] Fahimirad S, Abtahi H, Satei P, Ghaznavi-Rad E, Moslehi M, Ganji A. Wound healing performance of PCL/CS based electrospun nanofiber electrosprayed with CCM loaded CS nanoparticles. Carbohydr Polym. 2021;259:117640.
[15] Patrulea V, Ostafe V, Borchard G, Jordan O. CS as a starting material for wound healing applications. Eur J Pharm Biopharm. 2015;97:417-426.
[16] Biranje S, Madiwale P, Adivarekar RV. Electrospinning of CS/PVA nanofibrous membrane at ultralow solvent concentration. J Polym Res. 2017;24:1-10.
[17] Harpaz D, Axelrod T, Yitian AL, Eltzov E, Marks RS, Tok AI. Dissolvable polyvinyl-alcohol film, a time-barrier to modulate sample flow in a 3D-printed holder for capillary flow paper diagnostics. Materials. 2019;12(3):343.
[18] Peng L, Zhou Y, Lu W, Zhu W, Li Y, Chen K, Zhang G, Xu J, Deng Z, Wang D. Characterization of a novel PVA/CS porous hydrogel combined with bone marrow mesenchymal stem cells and its application in articular cartilage repair. BMC Musculoskelet Disord. 2019;20:257.
[19] Nathan KG, Genasan K, Kamarul T. PVA-CS scaffold for tissue engineering and regenerative medicine application: a review. Marine Drugs. 2023;21(5):304.
[20] Chetouani A, Elkolli M, Bounekhel M, Benachour D. CS/oxidized pectin/PVA blend film: Mechanical and biological properties. Polym. Bull. 2017;74:4297–4310.
[21] Fahimirad S, Abtahi H, Satei P, Ghaznavi-Rad E, Moslehi M, Ganji A. Wound healing performance of PCL/CS based electrospun nanofiber electrosprayed with CCM loaded CS nanoparticles. Carbohydr Polym. 2021;259:117640.
[22] Singh H, Dhanka M, Yadav I, Gautam S, Bashir SM, Mishra NC, Hassan S. Technological interventions enhancing CCM bioavailability in wound-healing therapeutics. Tissue Eng Part B Rev. 2024;30(2):230-253.
[23] Vivcharenko V, Przekora A. Modifications of wound dressings with bioactive agents to achieve improved pro-healing properties. Appl Sci. 2021;11(9):4114.
[24] Akbik D, Ghadiri M, Chrzanowski W, Rohanizadeh R. CCM as a wound healing agent. Life Sci. 2014;116(1):1-7.
[25] Salehi M, Farzamfar S, Ehterami A, Paknejad Z, Bastami F, Shirian S, Vahedi H, Koehkonan GS, Goodarzi A. Kaolin-loaded CS/PVA electrospun scaffold as a wound dressing material: In vitro and in vivo studies. J Wound Care. 2020;29(5):270-280.
[26] Dhurai B, Saraswathy N, Maheswaran R, Sethupathi P, Vanitha P, Vigneshwaran S, and Rameshbabu V. Electrospinning of CCM loaded CS/poly (lactic acid) nanofilm and evaluation of its medicinal characteristics. Front Mat Sci. 2013;7:350-361.
[27] Li Y, Zhu J, Cheng H, Li G, Cho H, Jiang M, Gao Q, Zhang X. Developments of advanced electrospinning techniques: A critical review. Adv Mater Technol. 2021;6(11):2100410.
[28] Thuy NTT, Ghosh C, Hwang S-G, Lam DT, Park JS. Characteristics of CCM-loaded poly (lactic acid) nanofibers for wound healing. J Mater Sci. 2013;48:7125-7133.
[29] Sedghi R, Shaabani A. Electrospun biocompatible core/shell polymer-free core structure nanofibers with superior antimicrobial potency against multi drug resistance organisms. Polymer. 2016;101:151-157.
[30] Mahmud MM, Zaman S, Perveen A, Jahan RA, Islam MF, Arafat MT. Controlled release of CCM from electrospun fiber mats with antibacterial activity. J Drug Deliv Sci Technol. 2020;55:101386.